

An easy access to an organometallic low molecular weight gelator: a crystal engineering approach

Pathik Sahoo, D. Krishna Kumar, Darshak R. Trivedi, Parthasarathi Dastidar^{*}

Department of Organic Chemistry, Indian Association for the Cultivation of Science, 2A & 2B Raja S. C. Mullick Road, Jadavpur, Kolkata 700 032, West Bengal, India

Received 20 January 2008; revised 11 March 2008; accepted 12 March 2008

Available online 15 March 2008

Abstract

In this Letter, a crystal engineering rationale is exploited to achieve an easy access to an organometallic *low molecular weight gelator* (LMWG) derived from a salt of ferrocene-1,1'-dicarboxylic acid (FDCA) and dicyclohexyl amine (DCHA). To the best of our knowledge, this is the first report wherein a crystal engineering approach has been exploited to design an organometallic LMWG. © 2008 Elsevier Ltd. All rights reserved.

Low molecular weight gelators (LMWGs)¹—compounds able to gel various organic (organogel) and aqueous (hydrogel) solvents—are an important class of compounds due to their various potential applications.¹ However, the mechanism of gel formation is poorly understood. Since entangled network of one dimensional (1D) fibers, termed *self-assembled fibrillar networks* (SAFINS),¹ are often seen in the gel samples via various microscopic techniques, it is argued that anisotropic interactions that encourage the gelator molecules to self-assemble in 1D might promote gelation.² Encouraged by this idea, we have exploited crystal engineering³ concepts to design and synthesize various classes of LMWGs.⁴ Although a rich variety of LMWG of organic origin are known in the literature,¹ reports on organometallic LMWG are scarce despite having potential applications in organometallics in synthesis, catalysis and materials chemistry (Chart 1).⁵ However, the methods available for the synthesis of organometallic LMWG are cumbersome.

Since ferrocene (Fc) is a well-known redox centre, it has already been incorporated in polymeric gel matrices for bio-sensing applications,⁶ and its antibiotic properties in

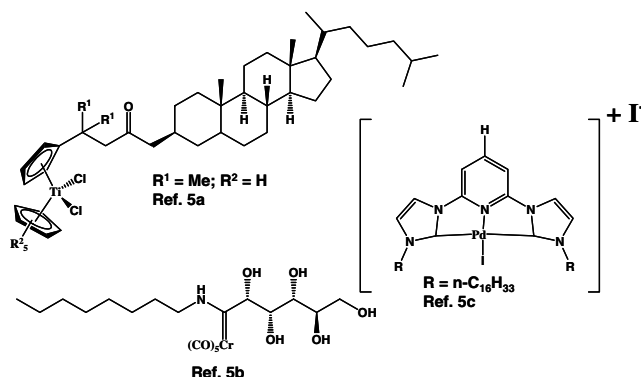


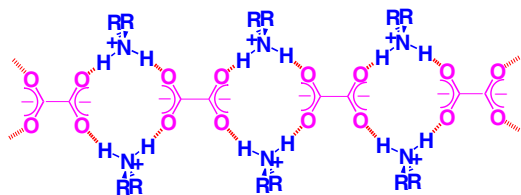
Chart 1. Organometallic LMWGs reported to date.

some polypeptides⁷ and catalytic properties in carbon nanotube production⁸ have also been reported. However, there are no ferrocene containing LMWG reported to date.

Recently, we identified a supramolecular synthon derived from secondary ammonium dicarboxylate (SAD) salts that imparts a 1D hydrogen bonded network (HBN) thereby facilitating gelation⁹ (Scheme 1). In this Letter, we have exploited the SAD synthon to effect an easy synthesis of a ferrocene (Fc)-based organometallic LMWG. For this purpose, we chose 1:2 (acid/amine) salt of ferrocene-1,1'-dicarboxylic acid (FDCA) and dicyclohexyl

^{*} Corresponding author.

E-mail addresses: parthod123@rediffmail.com, ocpd@iacs.res.in (P. Dastidar).



Scheme 1. 1D network in secondary ammonium dicarboxylate.

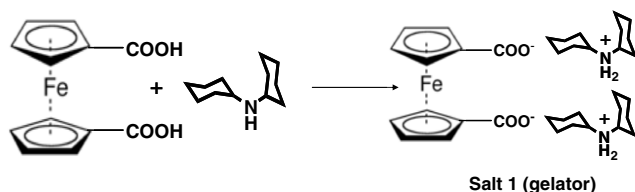
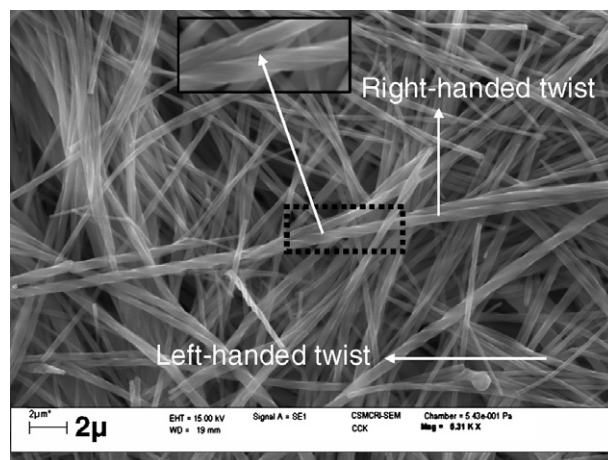


Chart 2. Organometallic LMWG reported herein.

amine (DCHA) because the 1:2 (acid/amine) SAD salt should display a 1D HBN as demonstrated by us⁹ (Scheme 1) and may, therefore, show gelation abilities. When the dibasic acid FDCA was reacted with DCHA in methanol in a 1:2 (acid/amine) molar ratio, bis-dicyclohexylammonium ferrocene-1,1'-dicarboxylate salt **1** was produced in near quantitative yield (Chart 2).¹⁰

The presence of COO^- (1561 cm^{-1}) and the absence of COOH (1677 cm^{-1} of FDCA) in the FT-IR clearly indicated the formation of salt **1**. Salt **1** turned out to be a good gelator of various organic solvents which was evident from its minimum gelator concentration (MGC) (1.3–4.1 wt %) and gel dissociation temperature (T_{gel}) (48–119 °C) (Table 1). Scanning electron microscopy (SEM) of the DMF derived xerogel of **1** revealed the presence of several micrometer long entangled fibrous networks comprising twisted fibers of both handedness (Fig. 1).

When analytically pure salt **1** was crystallized from 1,2-dichlorobenzene, crystals having two different morpholo-

Fig. 1. SEM micrograph of the DMF-xerogel (2 wt %) of salt **1** displaying entangled fibers having both handedness; inset depicts the right-handedly twisted fibers.

gies (block and needle) were obtained, which were subjected to single crystal X-ray diffraction.¹¹ Whilst the needle-shaped crystals turned out to be 1:2 salt **1**, the block-shaped crystal was found to be 1:1 salt **2**. In the crystal structure of **1**, the COO^- functionalities are oriented almost in an *anti* fashion and were involved in hydrogen bonding interactions with the cationic moieties via $\text{N-H}\cdots\text{O}$ interactions [$\text{N}\cdots\text{O} = 2.661(6)\text{--}2.706(6)\text{ \AA}$; $\angle\text{N-H}\cdots\text{O} = 157.1\text{--}161.9^\circ$] so that a cyclic network was formed. Since the anionic moiety is a dicarboxylate, the network was propagated in 1D giving rise to the HBN as envisaged in the SAD salts (Scheme 1) (Fig. 2a). These results clearly demonstrated the importance of the 1D HBN in the gelation process. On the other hand, in the crystal structure of salt **2**, COO^- is involved in hydrogen bonding interactions with the cationic species via $\text{N-H}\cdots\text{O}$ interactions [$\text{N}\cdots\text{O} = 2.721(2)\text{--}2.811(2)\text{ \AA}$; $\angle\text{N-H}\cdots\text{O} = 157(2)\text{--}170(2)^\circ$] resulting in a cyclic network. The COOH group, on the other hand, forms hydrogen

Table 1
Gelation data for salts **1** and **2**

Solvent	Salt 1			Salt 2	
	BP (°C)	MGC (wt %)	T_{gel}^a (°C)	MGC (wt %)	T_{gel}^a (°C)
DMSO	189–193	1.3	48	1.56	47
DMF	153	1.7	70	1.76	53
Methyl salicylate	220–224	3.2	83	—	—
Ph-NO ₂	210	1.8	69	—	—
Ph-H	79–80	2.6	90	—	—
Ph-Cl	130–133	2.9	104	—	—
Ph-Br	154–158	3.1	98	—	—
Ph-Me	110	2.7	108	—	—
1,2-Dichlorobenzene	177	4.0	60	—	—
CCl ₄	76–77	4.1	80	—	—
<i>o</i> -Xylene	142–145	1.3	85	—	—
<i>m</i> -Xylene	138	4.0	119	—	—
<i>p</i> -Xylene	137	3.2	110	—	—
Mesitylene	163–165	3.3	113	—	—

^a T_{gel} was measured using the dropping ball method.

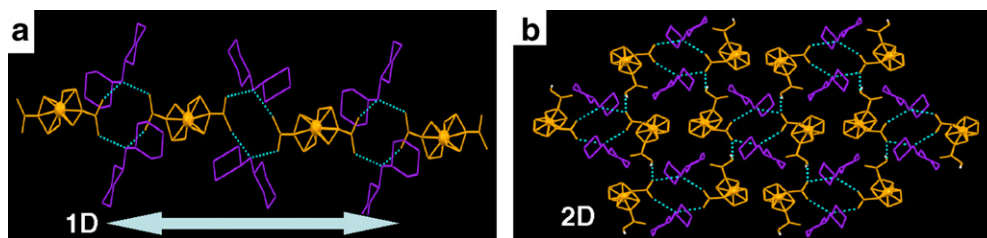


Fig. 2. Illustration of single crystal structures; (a) 1D HBN in salt **1**; (b) 2D HBN in salt **2**.

bonding contacts with COO^- [$\text{O}\cdots\text{O} = 2.590(2) \text{ \AA}$; $\angle\text{O}-\text{H}\cdots\text{O} = 161(4)^\circ$] from the neighbouring anionic species leading to an overall 2D HBN (Fig. 2b). Since 2D HBN either promote weak gelation or no gelation at all,² salt **2** was prepared in bulk (1696 cm^{-1} and 1536 cm^{-1} for the $\text{C}=\text{O}$ stretching of COOH and COO^- , respectively) in order to study its gelation behaviour. Since the COO^- group is hydrogen bonded with both the ammonium $\text{N}-\text{H}$ and COOH , its characteristic stretching band appears at 1536 cm^{-1} which is 25 cm^{-1} less than that of the COO^- in salt **1** wherein it is only hydrogen bonded with the ammonium $\text{N}-\text{H}$. Gelation data of salt **2** clearly indicated its nongelling behaviour except two solvents DMF and DMSO. Thus, these results corroborate well with the single crystal structures of salts **1** and **2**.

However, further investigation revealed interesting events. It was observed that the simulated XRPD pattern of salt **1**, except for some major peaks, did not exactly match with that of the bulk solid.¹² This could be either due to the less crystalline nature of the bulk solid or a predominant crystalline morph that is different from that of the single crystal of salt **1** that was subjected to X-ray diffraction. It may be emphasized here that the HBN in the crystalline phase of the bulk may still be 1D as observed in the single crystal structure of salt **1**, only the packing of such a network may be different. The most interesting observation, however, was the near identical XRPD patterns of the DMF-xerogels of salts **1** and **2** which were also identical with that of the bulk solid of salt **1** (Fig. 3).

This indicated the formation of salt **1** from salt **2** during the process. Attempts to establish that the formation of salt **1** from salt **2** actually took place during gel formation of salt **2** was inconclusive because a broad peak between 1500 and 1800 cm^{-1} appeared in the IR spectrum of the DMF-gel of salt **2**. On the other hand, the existence of salt **1** in the DMF-xerogel of salt **2** was supported by the presence of an IR band at 1570 cm^{-1} ($\text{C}=\text{O}$ stretching of COO^-). Close observation of a DMF-xerogel of salt **2** prepared on a glass slide revealed a remarkable colour difference between the centre (yellow) and peripheral (brown) regions. IR experiments established the existence of salt **1** (1570 cm^{-1} , COO^-) and FDCA (1678 cm^{-1} , COOH) in the centre and peripheral regions, respectively (Fig. 4).

Since the X-ray beam falls at the centre of the sample holder, it was not surprising that the XRPD pattern of the DMF-xerogel of salt **2** matched with that of the xerogel

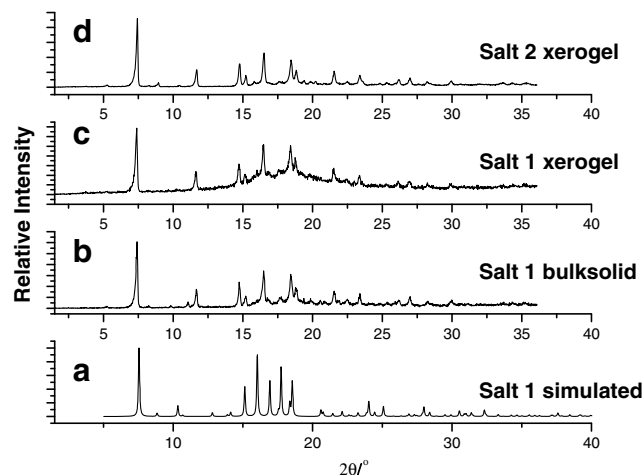


Fig. 3. XRPD patterns of salts **1** and **2** under various conditions, (a) simulated from single crystal data, (b) bulk solid as synthesized, (c) DMF-xerogel; (d) DMF-xerogel of salt **2**.

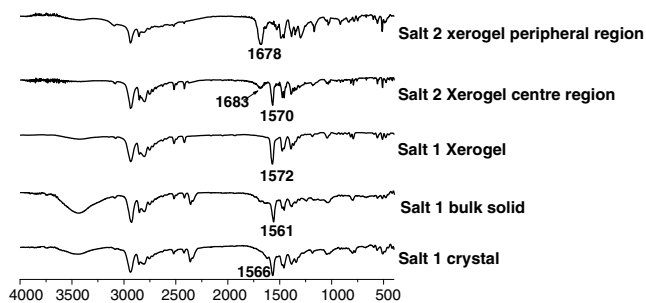


Fig. 4. FT-IR spectra of salts **1** and **2** under various conditions.

and bulk solid of salt **1**. The morphology of the fibers in the DMF-xerogel of salt **2** as revealed in SEM was found to be nearly identical with that obtained from salt **1**, further supporting the presence of the gelator salt **1** in the DMF-xerogel of salt **2** (Fig. 5). Thus, these results clearly indicated the transformation of salt **2** to salt **1** during the process of xerogel formation. Whether such a transformation took place during gel formation or not could not be established from the IR data as mentioned above. However, this does not rule out the possibility of such a transformation during gel formation as well.

This report clearly highlights the merit of the crystal engineering approach which enabled us to achieve an easy access to an organometallic LMWG, namely salt **1**. The

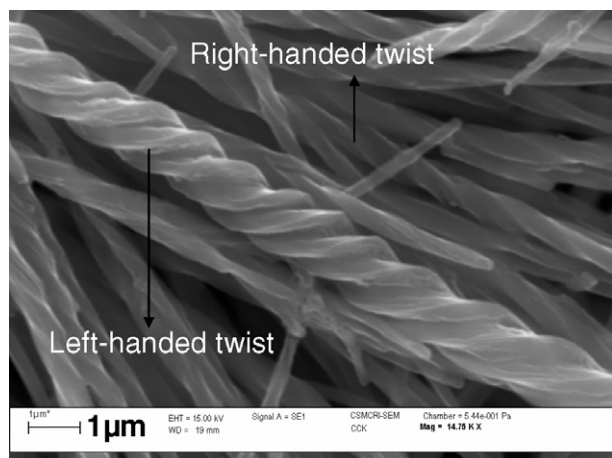


Fig. 5. SEM micrograph of the DMF-xerogel of salt **2** (2 wt%) displaying remarkable similarity with that obtained from salt **1** (see Fig. 1).

gelator salt **1** showed excellent gelation properties with various organic fluids and the 1D hydrogen bonded network present in its single crystal structure corroborates well with the rationale with which the gelator molecule was designed. Incorporation of a ferrocene moiety in the gelator may lead to new applications. Efforts are underway to discover new LMWGs containing ferrocene, which could be used for various materials applications.

Acknowledgement

P.S. thanks CSIR, New Delhi, for a Junior Research Fellowship (JRF).

References and notes

1. *Molecular Gels. Materials with Self-Assembled Fibrillar Networks*; Weiss, R. G., Terech, P., Eds.; Springer: Dordrecht, The Netherlands, 2005.
2. (a) Luboradzki, R.; Gronwald, O.; Ikeda, M.; Shinkai, S.; Reinhoudt, D. N. *Tetrahedron* **2000**, *56*, 9595–9599; (b) Tamaru, S.-i.; Luboradzki, R.; Shinkai, S. *Chem. Lett.* **2001**, 336–337; (c) van Esch, J. H.; Feringa, B. L. *Angew. Chem., Int. Ed.* **2000**, *39*, 2263–2266.
3. (a) Desiraju, G. R. *Crystal Engineering: The Design of organic solids*; Elsevier: Amsterdam, 1989; (b) Desiraju, G. R. *Angew. Chem., Int. Ed. Engl.* **1995**, *34*, 2311–2327.
4. (a) Ballabh, A.; Trivedi, D. R.; Dastidar, P. *Chem. Mater.* **2003**, *15*, 2136–2140; (b) Trivedi, D. R.; Ballabh, A.; Dastidar, P.; Ganguly, B. *Chem.-Eur. J.* **2004**, *10*, 5311–5322; (c) Trivedi, D. R.; Ballabh, A.; Dastidar, P. *J. Mater. Chem.* **2005**, *15*, 2606–2614; (d) Trivedi, D. R.; Ballabh, A.; Dastidar, P. *Cryst. Growth Des.* **2006**, *6*, 763–768; (e) Trivedi, D. R.; Dastidar, P. *Chem. Mater.* **2006**, *18*, 1470–1478; (f) Ballabh, A.; Trivedi, D. R.; Dastidar, P. *Org. Lett.* **2006**, *8*, 1271–1274; (g) Trivedi, D. R.; Dastidar, P. *Cryst. Growth Des.* **2006**, *6*, 1022–1026; (h) Ballabh, A.; Trivedi, D. R.; Dastidar, P. *Chem. Mater.* **2006**, *18*, 3795–3800; (i) Adarsh, N. N.; Krishna Kumar, D.; Dastidar, P. *Tetrahedron* **2007**, *63*, 7386–7396.
5. (a) Klawonn, T.; Gansäuer, A.; Winkler, I.; Lauterbach, T.; Franke, D.; Nolte, R. J. M.; Feiters, M. C.; Börner, H.; Hentschel, J.; Dötz, K. H. *Chem. Commun.* **2007**, 1894–1895; (b) Bühler, G.; Feiters, M. C.; Nolte, R. J. M.; Dötz, K. H. *Angew. Chem., Int. Ed.* **2003**, *42*, 2494–2497; (c) Tu, T.; Assenmacher, W.; Peterlik, H.; Weisbarth, R.; Nieger, M.; Dötz, K. H. *Angew. Chem., Int. Ed.* **2007**, *46*, 6368–6371.
6. (a) Bu, H.-j.; Mikkelsen, S. R.; English, A. M. *Anal. Chem.* **1995**, *67*, 4071–4076; (b) Calvo, E. J.; Danilowicz, C.; Diaz, L. J. *Chem. Soc., Faraday Trans.* **1993**, *89*, 377–384.
7. Chantson, J. T.; Falzacappa, M. V. V.; Crovella, S.; Metzler-Nolte, N. *ChemMedChem* **2006**, *1*, 1268–1274.
8. (a) Qiu, J.; An, Y.; Zhao, Z.; Li, Y.; Zhou, Y. *Fuel Process. Technol.* **2004**, *85*, 913–920; (b) Xie, S.; Song, L.; Ci, L.; Zhou, Z.; Dou, X.; Wang, G.; Sun, L. *Sci. Tech. Adv. Mater.* **2005**, *6*, 725–745.
9. (a) Ballabh, A.; Trivedi, D. R.; Dastidar, P. *Cryst. Growth Des.* **2005**, *5*, 1545–1553; (b) Trivedi, D. R.; Ballabh, A.; Dastidar, P. *Cryst. Growth Des.* **2006**, *6*, 763–768.
10. Synthesis of bis-dicyclohexylammonium ferrocene-1,1'-dicarboxylate (**salt 1**): A methanolic (~20 ml) solution of ferrocene-1,1'-dicarboxylic acid (0.3649 mmol, 100.0 mg) was added dropwise to a flask containing dicyclohexyl amine (0.72968 mmol, 132.3 mg). The reaction mixture was stirred for 3 h followed by solvent removal on a rotary evaporator. The resultant solid was isolated by washing with *n*-hexane followed by filtration in almost quantitative yield. Mp 180–182 °C (charred); Anal. Calcd for $C_{24}H_{33}N_2O_4Fe$: C, 67.91; H, 8.87; N, 4.40. Found: C, 67.76; H, 8.55; N, 4.47; FT-IR (KBr) cm^{-1} : 3448, 2938, 2855, 2806, 2756, 2520, 2421, 2360, 1619, 1561, 1478, 1459, 1384, 1342, 1183, 1048, 918, 796, 775, 671, 595, 562, 509, 418. Synthesis of dicyclohexylammonium hydrogen ferrocene-1,1'-dicarboxylate (**salt 2**): A methanolic (~15 ml) solution of ferrocene-1,1'-dicarboxylic acid (0.5473 mmol, 150.0 mg) was added dropwise to a flask containing dicyclohexyl amine (0.5476 mmol, 99.3 mg). The reaction mixture was stirred for 25 min followed by solvent removal using a rotary evaporator. The resultant solid was isolated by washing with *n*-hexane followed by filtration in almost quantitative yield. Mp 182–186 °C (charred); Anal. Calcd for $C_{24}H_{33}NO_4Fe$: C, 63.3; H, 7.3; N, 3.02. Found: C, 63.69; H, 7.43; N, 3.33; FT-IR (KBr) cm^{-1} : 3433, 3105, 2934, 2862, 2570, 2365, 2344, 1696, 1616, 1536, 1464, 1384, 1348, 1249, 1182, 1151, 1037, 1020, 992, 924, 833, 813, 787, 725, 595, 550, 483, 448, 425.
11. *Single crystal X-ray diffraction*: Crystal data for salt **1** (FDCA-2D-CHA): $C_{36}H_{56}FeN_2O_4$, FW = 636.68, tetragonal, $P4_2/n$, $a = 16.5254(8)$, $b = 16.5254(8)$, $c = 12.4792(12)$ Å, $V = 3407.9(4)$ Å³, $Z = 4$, $D_c = 1.241$ g cm⁻³, $F(000) = 1376$, $T = 100(2)$ K, final residuals (for 195 parameters) were $R_1 = 0.1128$ for 2680 reflections with $I > 2\sigma(I)$ and $R_1 = 0.1325$, $wR_2 = 0.2256$, GOF = 1.246 for all 3165 reflections. Crystal data for salt **2** (FDCA-DCHA): $C_{24}H_{33}FeNO_4$, FW = 455.36, monoclinic, $P2_1/c$, $a = 9.4398(11)$, $b = 14.9347(17)$, $c = 15.8964(18)$ Å, $\beta = 95.323(2)$, $V = 2231.4(4)$ Å³, $Z = 4$, $D_c = 1.355$ g cm⁻³, $F(000) = 968$, $T = 100(2)$ K. Final residuals (for 403 parameters) were $R_1 = 0.0483$ for 4359 reflections with $I > 2\sigma(I)$ and $R_1 = 0.0599$, $wR_2 = 0.1194$, GOF = 1.052 for all 5189 reflections. [CCDC 666733 and 666734 contain the supplementary crystallographic data for this paper. These data can be obtained free of charge from The Cambridge Crystallographic Data Centre via www.ccdc.cam.ac.uk/data_request/cif.
12. *X-ray powder diffraction (XRPD)*: XRPD patterns for the bulk solids and xerogels for the salts **1** and **2** were recorded on XPERT Philips (CuK α radiation, $\lambda = 1.5418$ Å) at a scan speed of 0.01°/s in 2θ . The sample holder was filled with homogeneously powdered samples for data collection of the bulk solid. For xerogel data collection, the sample holder was filled with the gel which was then evaporated under vacuum in a desiccator prior to data collection.